Exclusion of Noncrystalline Polymer from the Interlamellar Region in Poly(vinylidene fluoride)/Poly(methyl methacrylate) Blends

Hiromu Saito† and Bernd Stühn*

Fakultät für Physik, Universität Freiburg, Hermann-Herder Strasse 3, D-79104 Freiburg, Germany

Received June 16, 1993; Revised Manuscript Received October 13, 1993®

ABSTRACT: We investigated the intraspherulitic structure of poly(vinylidene fluoride) (PVDF)/poly(methyl methacrylate) (PMMA) blends using polarized microscopy and small-angle X-ray scattering (SAXS). The structure of the spherulite is coarser with increasing crystallization temperature. The internal crystallinity obtained by SAXS is much larger than its overall value derived from DSC for the coarse spherulite, indicating that the amorphous region between lamellar bundles is large in this structure. For coarser structures, the electron density difference between the crystalline and the amorphous phase, obtained from an analysis of SAXS scattering profiles, is lower. That is, the concentration of PMMA in the interlamellar amorphous region is low in the coarse spherulite. This suggests that PMMA is partially excluded from the interlamellar region in the coarse spherulite.

In mixtures of crystalline and noncrystalline components, the noncrystalline component must diffuse away from a crystal growth front; i.e., exclusion should take place. The exclusion effect is well-known in polymer/diluent systems.[1-6] When the diluent can rapidly diffuse away from a growing spherulite due to its large mobility, a concentration gradient is established at the growth front. The existence of the concentration gradient has been confirmed by the concentration distribution observed by ultraviolet microscopy[5,6] and indirectly by the growth rate depending on the distribution of spherulites.[4] Because of the existence of the concentration gradient, the crystallization kinetics is nonlinear; i.e., the spherulitic growth rate is constant at the beginning, but it decreases at the late stages.[1-4]

On the other hand, in polymer/polymer systems, the mobility of the noncrystalline polymer is small. Thus the noncrystalline polymer seems to be excluded only on the length scale of lamellar bundles, at most. Keith and Padden have suggested that the spherulite becomes coarse and open when the noncrystalline polymer diffuses out of the interlamellar region and is trapped in pockets between lamellar bundles.[1,2,7-9] However, the exclusion effect on the sperulitic structure has not been demonstrated experimentally.

Experimentally, the exclusion will be elucidated by investigating the effect of the intraspherulitic structure on the compactness of the spherulite. Typically, adding the noncrystalline polymer or raising the crystallization temperature causes the spherulitic morphology to become coarser and more open, while reducing the fraction of noncrystalline polymer or dropping the crystallization temperature causes it to become more compact. In this paper, the spherulite of a poly(vinylidene fluoride) (PVDF)/poly(methyl methacrylate) (PMMA) blend, having different compactness at the same blend composition, is prepared by crystallization at different temperatures. The spherulite morphology is characterized with polarized light microscopy and the intraspherulitic structure is investigated by small-angle X-ray scattering (SAXS).

The polymer specimens used in this study were commercial polymers. PVDF was supplied by Polyscience, Inc.; M_w = 60 000. PMMA was supplied by Röhm GmbH; M_w = 58 000.

PVDF and PMMA were dissolved at 10 wt % of the total polymer in *N*,*N*-dimethylacetamide (DMAc). The solution was cast onto a cover glass. After the solvent had been evaporated at room temperature, the cast film was dried further under vacuum (10^{-4} mmHg) for 3 days at room temperature. The thin film thus prepared was used for optical microscopy and DSC experiments. A stack of thin-cast film was compression-molded at 210 °C using a molder of 17-mm length and 5-mm width into a thick film of about 1-mm thickness. This thick film was used for the SAXS studies. The specimen was melted at 210 °C for 10 min under pressure and then cooled to the desired crystallization temperature at a cooling rate of 20 °C/min. Crystallization was carried out for 24 h to ensure complete crystallization, i.e., volume-filled spherulites. After crystallizing, the specimen was quenched in a water bath.

The spherulitic morphology was observed by a Leitz II Pol-BK polarized microscope equipped with a 35-mm camera (Type A-E, Leica). DSC thermograms were recorded using a Perkin-Elmer DSC-4 at a heating rate of 20 K/min. The SAXS measurements were performed in an evacuated Kratky compact camera (Type KKK, Anton Paar K.G.) using an 80-μm entrance slit. The radiation of a Cu anode (Siemens X-ray tube FK 60-20) was reflected from a graphite monochromator to obtain monochromatic Cu Kα radiation with a wavlength λ = 0.154 nm. The generator was operated at 40 kV and 50 mA. The scattered intensity was detected by a scintillation counter in a step scanning mode and was stored on a computer. The measurement was carried out at 20 °C. The scattering profiles were corrected for background scattering and desmeared using Strobl's method.[10] Then, the scattering caused by the thermal density fluctuation was eliminated by evaluating the slope of a Iq^4 versus q^4 plot at high scattering vectors, $q = (4\pi/\lambda)\sin(\theta/2)$ where θ is the scattering angle.[11]

Typical spherulitic morphologies of PVDF/PMMA blends are shown in Figure 1. In neat PVDF, compact spherulites having a clear Maltese cross pattern are observed (Figure 1a). Similarly compact spherulites are also developed in the blend crysallized at a low crystal-

† Present address: Department of Organic & Polymeric Materials, Tokyo Institute of Technology, Ookayama, Meguro-ku, Tokyo 152, Japan.

® Abstract published in *Advance ACS Abstracts*, November 15, 1993.

0024-9297/94/2227-0216$04.50/0

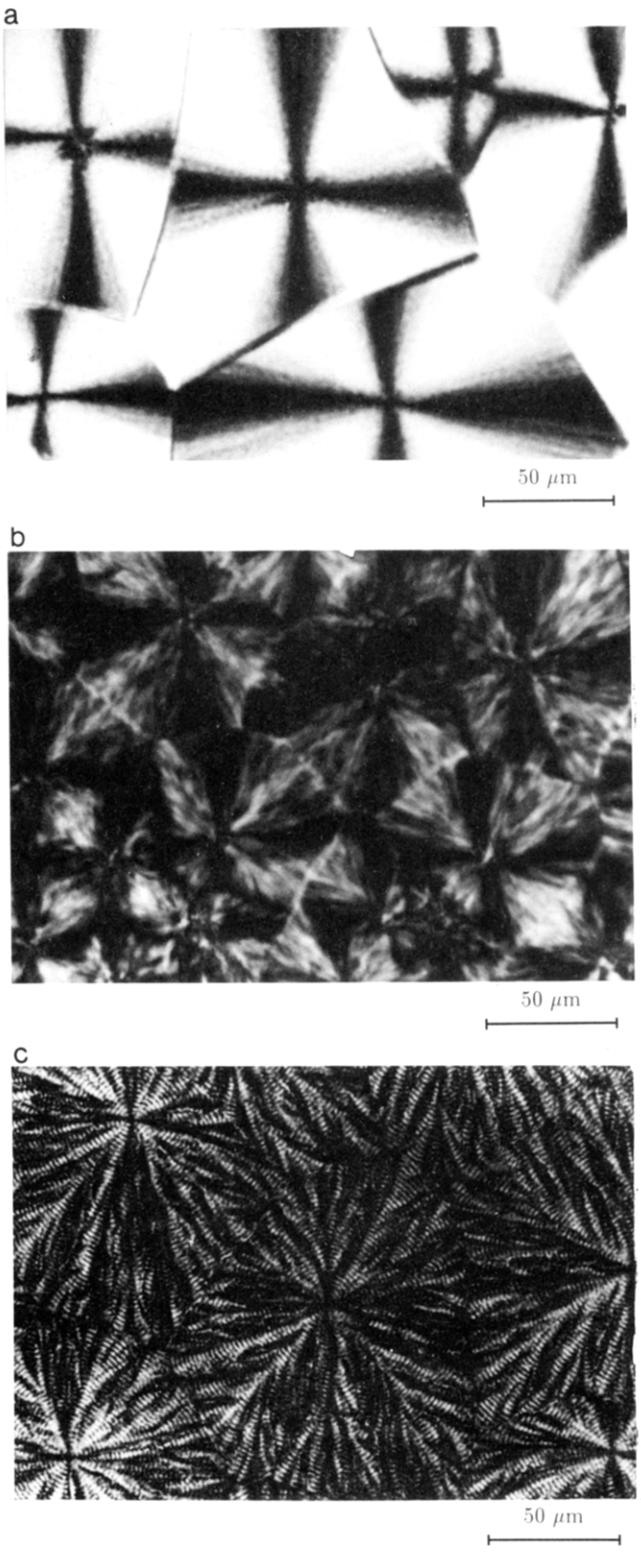

Figure 1. Optical micrographs: (a) PVDF/PMMA 100/0 crystallized at 160 °C; (b) compact spherulite; PVDF/PMMA 60/40 crystallized at 145 °C; (c) coarse spherulite; PVDF/PMMA 60/40 crystallized at 153 °C.

lization temperature (Figure 1b). However, the Maltese cross pattern is diffuse compared to that of neat PVDF; i.e., there is a mottling of the regions where light is transmitted at 0° and 90°. The diffuse Maltese cross pattern may be ascribed to the randomness of the orientation of lamellar bundles. In the blend crystallized at higher temperatures (above 150 °C in this composition), coarse spherulites are developed. They consist of lamellar bundles of large cross section, and the Maltese cross pattern

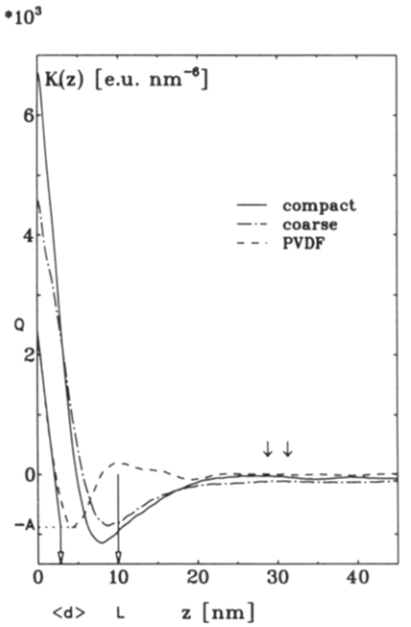

Figure 2. Correlation functions $K(z)$ derived from SAXS.

is completely lost (Figure 1c). The spherilutes are also banded.[12,13] Their coarseness may be caused by the exclusion of PMMA from the lamellar bundles. The excluded PMMA hinders the radial growth of the crystalline lamellae, as suggested by Morra and Stein.[12] The intraspherulitic structure of these three textures was investigated by SAXS measurement.

To discuss the intraspherulitic structure based on the SAXS results, it is convenient to employ the Fourier transformation of the scattering curve, i.e., to calculate the linear correlation function $K(z)$ defined by[14,15]

$$K(z) = \frac{1}{2\pi^2}\int_0^\infty q^2 I(q) \cos qz \, dq \tag{1}$$

The correlation function $K(z)$ thus obtained is shown in Figure 2. In the application of the transformation eq 1 to the SAXS data it is important to determine the scattering profile up to large enough q and subtract the scattering due to density fluctuations in order to avoid cutoff errors. $K(z)$ is related to the electron density distribution $\rho(z)$, so that the parameters of the intraspherulitic structure can be obtained from the shape of the $K(z)$.[14,15] The meaning of the parameters is indicated in Figure 2 for the example of the measurement on pure PVDF.

The position of the first maximum (arrows in Figure 2) indicates the long spacing L, which means the most probable next-neighbor distance of the lamellae. The extrapolation of the initial slope for the $K(z)$ intersects the base line $K(z) = -A$ at $z = \langle d \rangle$, the average thickness of the crystalline region. Here the base line is the horizontal line for the plateau region of the first minimum of $K(z)$ and the slope $dK(z)/dz$ is given by

$$\frac{dK(z)}{dz} = -\frac{Q + A}{\langle d \rangle} \tag{2}$$

where Q is the invariant which is obtained by extrapolating $K(z)$ to $z = 0$.

From the values of $\langle d \rangle$ and L, the linear crystallinity w_l is obtained:[11,16-18]

$$w_l = \langle d \rangle / L \tag{3}$$

On the other hand, the average crystallinity within lamellar

Table 1. Thickness of the Crystalline Region $\langle d \rangle$, the Long Spacing L, and the Resulting Thickness of the Amorphous Region AM for *Pure* PVDF and Both Spherulite Structures of the Blend

	$\langle d \rangle$ (nm)	L (nm)	AM (nm)
PVDF[a]	2.8	10.0	7.2
compact[b]	5.4	28.0	22.6
coarse[c]	7.1	30.5	23.4

[a] Neat PVDF crystallized at 160 °C. [b] Compact spherulite of blend; PVDF/PMMA 60/40 crystallized at 145 °C. [c] Coarse spherulite of blend; PVDF/PMMA 60/40 crystallized at 153 °C.

Table 2. Values for the Crystallinity w_l (Eq 3) and w_o (from DSC) and the Compactness Parameter α (See Text)[a]

	w_l	w_o	α	Q (eu nm^{-6})	$(\eta_c - \eta_a)^2$ (eu nm^{-6})
PVDF	0.28	0.28[b]	1	2420	12 000
compact	0.193	0.118	0.61	7800	82 100
coarse	0.233	0.120	0.51	4880	53 500

[a] The electron density difference $\mu_c - \mu_a$ is obtained from Q according to eq 5. [b] This value was normalized by that of u.

bundles w_i is given by[14]

$$w_i = A/(A + Q) \tag{4}$$

Since the base line was not identical in the blends, A and $\langle d \rangle$ were obtained from eqs 2–4 by assuming $w_l = w_i$. The average thickness of the crystalline region $\langle d \rangle$, the long spacing L, and the thickness of the amorphous phase AM, obtained as $AM = L - \langle L \rangle$, are shown in Table 1. Note here that the addition of noncrystalline polymer causes an increase in the thickness of the AM. This suggests that the noncrystalline polymer is incorporated between the crystalline lamellae, as already demonstrated in refs 11 and 16–18. However, the details should be discussed in terms of the electron density difference, as demonstrated later.

In Table 2 we show the linear crystallinity w_l and the crystallinity w_o obtained by DSC. The w_o is the overall crystallinity, while the w_l is the internal crystallinity within the lamellar bundles. Thus a ratio of these values, $\alpha = w_o/w_l$, should be a measure for the compactness of spherulite if the specimen is completely volume-filled with spherulites. α increases as the amorphous region between lamellar bundles gets smaller (more compact), while it decreases as the amorphous region gets larger (more open). The result is shown in Table 2. The α of the coarse spherulite is smaller than that of the compact spherulite, indicating that the coarse spherulite is more open than the compact spherulite. According to Keith and Padden, the excluded noncrystalline polymer is trapped in the pockets between lamellar bundles in the open spherulite.[1,2,8,9] If the noncrystalline polymer is excluded in this manner, the concentration of the noncrystalline polymer will be lower in the amorphous phase between lamellae with decreasing compactness, while it will be higher in the pockets between lamellar bundles. In the following, the concentration of the noncrystalline polymer in the amorphous phase between lamellae will be discussed in terms of the electron density difference measured in SAXS.

Since the invariant Q is proportional to α, the mean-squared electron density difference between the crystalline and amorphous phases $(\eta_c - \eta_a)^2$ for an ideal two-phase system is given by[14]

$$(\eta_c - \eta_a)^2 = Q/\alpha w_l(1 - w_l) \tag{5}$$

Q and $(\eta_c - \eta_a)^2$ are shown in Table 2. For PVDF the observed electron density difference results in a mass density difference between the crystalline and the amorphous phase $\Delta\rho = 0.37$ g/cm^3 in accordance with values reported in the literature. The $(\eta_c - \eta_a)^2$ of the blends are much larger than that of neat PVDF. We note that the electron densities of neat polymer systems are $\eta_{a,PVDF} = 0.860$ mole/cm^3 and $\eta_{a,PMMA} = 0.643$ mole/cm^3.[19] Therefore, the large value of $(\eta_c - \eta_a)^2$ in the blends is ascribed to the small η_a due to the presence of PMMA in the interlamellar amorphous region. Most interesting here is that the $(\eta_c - \eta_a)^2$ of the coarse spherulite is smaller than that of the compact spherulite, indicating that η_a of the coarse spherulite is larger than that of the compact spherulite. That is, the concentration of PMMA in the interlamellar region is lower because the spherulite is more open in spite of the same blend composition. This finding suggests that PMMA is partially excluded from the interlamellar region in the coarse spherulite.

Thus, the partial exclusion of noncrystalline polymer in coarse spherulite has been proved. This may support the theory of Keith and Padden. The origin of the coarseness of the spherulite lies in the exclusion of noncrystalline polymer from the interlamellar region.[1,2] However, a more detailed discussion will have to take into account the specific interaction which restricts the exclusion.[20,21] Finally we remark that the thickness of the interfacial region between the crystalline and the amorphous phase increases from 0.4 nm in pure PVDF to 1.8 nm in the blend. Detailed properties of the interface will be discussed in a separate publication together with results from dielectric spectroscopy.[22]

Acknowledgment. We are grateful to Prof. G. R. Strobl for helpful discussion. H.S. thanks the Alexander von Humboldt Stiftung for supporting his postdoctoral study in Germany.

References and Notes

(1) Keith, H. D.; Padden, F. J., Jr. *J. Appl. Phys.* **1963**, *34*, 2409.
(2) Keith, H. D.; Padden, F. J., Jr. *J. Appl. Phys.* **1964**, *35*, 1270.
(3) Goldenfeld, N. *J. Cryst. Growth* **1987**, *84*, 601.
(4) Okada, T.; Saito, H.; Inoue, T. *Macromolecules* **1990**, *23*, 3865.
(5) Ryan, T. G.; Calvert, P. D. *Polymer* **1982**, *23*, 877.
(6) Calvert, P.; Billingham, N. C. *Applied Polymer Light Microscopy*; Elsevier Applied Science: New York, 1989; Chapter 7.
(7) Warner, F. P.; Macknight, W. J.; Stein, R. S. *J. Polym. Sci., Polym. Phys. Ed.* **1977**, *15*, 2113.
(8) Stein, R. S.; Khambatta, F. B.; Warner, F. P.; Russell, T.; Escala, A.; Balizer, E. *J. Polym. Sci., Polym. Symp.* **1978**, *63*, 313.
(9) Hudson, S. D.; Davis, D. D.; Lovinger, A. J. *Macromolecules* **1992**, *25*, 1759.
(10) Strobl, G. R. *Acta Crystallogr.* **1970**, *A26*, 367.
(11) Russell, T. P.; Ito, H.; Wignall, G. D. *Macromolecules* **1988**, *21*, 1703.
(12) Morra, B. S.; Stein, R. S. *J. Polym. Sci., Polym. Phys. Ed.* **1982**, *20*, 2261.
(13) Keith, H. D.; Padden, F. J., Jr.; Russell, T. P. *Macromolecules* **1989**, *22*, 666.
(14) Strobl, G. R.; Schneider, M. J.; Voigt-Martin, I. G. *J. Polym. Sci., Polym. Phys. Ed.* **1980**, *18*, 1361.
(15) Tanabe, Y.; Strobl, G. R.; Fischer, E. W. *Polymer* **1986**, *27*, 1147.
(16) Wenig, W.; Karasz, F. E.; MacKnight, W. J. *J. Appl. Phys.* **1975**, *46*, 4194.
(17) Khambatta, F. B.; Warner, F.; Russell, T. P.; Stein, R. S. *J. Polym. Sci., Polym. Phys. Ed.* **1976**, *14*, 1391.
(18) Russell, T. P.; Stein, R. S. *J. Polym. Sci., Polym. Phys. Ed.* **1983**, *21*, 999.
(19) Nakagawa, K.; Ishida, Y. *J. Polym. Sci., Polym. Phys. Ed.* **1973**, *11*, 2153.
(20) Alfonso, G. C.; Russell, T. P. *Macromolecules* **1986**, *19*, 1143.
(21) Stein, R. S. *Pure Appl. Chem.* **1991**, *63*, 941.
(22) Saito, H.; Stühn, B. *Polymer*, in press.